Advanced Composite Materials
Publication details, including instructions for authors and subscription information:
http://www.tandfonline.com/loi/tacm20

Mechanical properties of Si3N4/SiC-whisker-reinforced Si3N4 three-layer composites

Masahiro Kato , Takayuki Fukasawa & Yasuhiro Goto

Version of record first published: 02 Apr 2012.

To cite this article: Masahiro Kato , Takayuki Fukasawa & Yasuhiro Goto (2000): Mechanical properties of Si3N4/SiC-whisker-reinforced Si3N4 three-layer composites , Advanced Composite Materials, 9:1, 37-46

To link to this article: http://dx.doi.org/10.1163/156855100300132956

Adv. Composite Mater., Vol. 9, No. 1, pp. 37–46 (2000)

Mechanical properties of Si_3N_4/SiC-whisker-reinforced Si_3N_4 three-layer composites

MASAHIRO KATO, TAKAYUKI FUKASAWA and YASUHIRO GOTO

Power Supply Materials and Devices Laboratory, Corporate Research and Development Center, Toshiba Corporation, 1 Komukai Toshiba-cho, Saiwai-ku, Kawasaki 210-0901, Japan

Received 2 December 1998; accepted 20 April 1999

Abstract—The relationship between the mechanical properties of three-layer composites which consist of surface Si_3N_4 layers and an inner SiC-whisker-reinforced Si_3N_4 layer and the surface residual compressive stress was investigated. It was found that the mechanical properties, such as Vickers hardness, fracture toughness, and bending strength decreased with the thickness of the surface Si_3N_4 layers. On the other hand, the surface residual stress was measured and calculated by the finite element method (FEM). It was found that the surface compressive residual stress decreased with the thickness of the surface layers and also increased with the content of SiC whiskers. Based on comparison of the behaviors of the mechanical properties and surface compressive stress of layered composites to the surface layer thickness, it was thought that the improvements in the mechanical properties of the layered composites were caused by the surface compressive stress resulting from mismatch in the thermal expansion.

Keywords: Si_3N_4; SiC; whisker; composite; residual stress.

1. INTRODUCTION

Layered composites have been studied extensively in recent years because of their unique properties. Improvement of fracture strength by surface compressive stress is one of the characteristic features of the layered composites [1–7]. The incorporation of residual stresses in (Al_2O_3 + ZrO_2(unstabilized))/(Al_2O_3 + ZrO_2(stabilized)) three-layer composites [2–6] leads to strength improvements of 375 MPa at room temperature and 200 MPa at 750°C, as compared with the monolithic materials. Another feature is non-linear fracture behavior similar to that of the long-fiber composites [8–17]. A SiC-whisker/Si_3N_4 multilayered composite shows a fracture energy of more than 3000 J/m^2 [16], which is about twenty times that of monolithic Si_3N_4.

Still another feature is a synergistic effect by which conflicting properties are realized at the same time. Sialon/Si_3N_4 layered composite [17] and rare-earth silicate/SiC layered composites are expected to achieve oxidation resistance without reducing strength [18, 19]. In the same manner, covering SiC-whisker-reinforced Si_3N_4 with monolithic Si_3N_4 is thought to be effective in improving oxidation properties without reducing mechanical properties, because the oxidation properties of monolithic Si_3N_4 are superior to those of SiC-whisker-reinforced Si_3N_4 [20].

Therefore, in this study, we fabricated three-layer composites in which the surface layers were monolithic Si_3N_4 and the inner layer was SiC-whisker-reinforced Si_3N_4 composite, and investigated the relationship between mechanical properties and surface compressive stress due to the mismatch of the thermal expansion between Si_3N_4 and SiC-whisker-reinforced Si_3N_4. In particular, fracture strength values were measured, and also calculated by using the flitch beam model.

2. EXPERIMENTAL

2.1. Sample preparation

The starting powders were prepared by ball-mill mixing a commercial-grade Si_3N_4 powder (0.5 μm, SN-E10, Ube Industries, Ltd., Japan) with 5 wt% Y_2O_3 (0.1 μm, 99.9%, Shin-Etsu Chemical Co., Ltd., Japan) and 5 wt% $MgAl_2O_4$ (0.1 μm, Kojundo Chemicals Co., Ltd., Japan), as sintering additives, and SiC whiskers (TWS-400, Tokai Carbon Co., Ltd., Japan). The composition of the sintering additives was a typical one for high-strength Si_3N_4 [21]. The SiC whisker contents were 0 (monolithic Si_3N_4), 10, and 20 wt%. The ball-mill mixing was performed for 16 h using n-butanol as a liquid medium. After drying and filtration with a nylon sieve with an aperture size of 500 μm, the powder mixtures were cold-pressed at 25 MPa to obtain green bodies for monolayers. The green bodies for layered composites were obtained by filling monolithic, composite, and monolithic powders sequentially into a steel die followed by cold-pressing at 25 MPa. Finally, the green bodies were hot-pressed in a carbon die at a temperature of 1700°C under 30 MPa for 1 h in 0.1 MPa N_2. The total thickness of the layered composites was 3 mm, in spite of the surface layer thickness of 200, 500, and 1000 μm.

2.2. Evaluation

In order to evaluate the physical properties of the monolayers, the following measurements were performed. Densities were measured by Archimedes' method with distilled water as a medium. Young's modulus was measured by the ultrasonic pulse method. The thermal expansion coefficient was measured by using an optical coherent meter between room temperature and 1100°C. Thermal expansion coefficients were obtained in the direction perpendicular to the hot-pressed axis.

On the other hand, in order to evaluate the mechanical properties of the layered composites, hot-pressed billets were machined to rectangular bars. The size of the bars was 3 × 4 × 40 mm. Vickers hardness was measured by using a micro Vickers hardness tester (AVK-C2, Akashi Co., Ltd., Japan) at 30 kg for 15 s. Fracture toughness was measured by the indentation fracture (IF) method (JIS-Z8401). Before forming the indentor trace, samples were finely polished to an Ra roughness of 0.1 μm. An optical microscope (SMZ-V, Nikon Co., Ltd., Japan) was used to examine the crack length. Bending strength was evaluated by a 3-point bending test with a 30-mm span in accordance with JIS-1601 by means of a testing machine (Type 1361, Instron, Ltd., England). Microstructures of fracture surfaces were observed with a scanning electron microscope (T330 JEOL, Japan). Furthermore, surface residual stress was measured by using an X-ray diffraction machine (RINT 1500, Rigaku Co., Ltd., Japan) using the $\sin^2 \psi$ method and also calculated by the finite element method (FEM).

3. RESULTS AND DISCUSSION

3.1. Physical properties of monolayers

Table 1 shows the physical properties, such as density, Young's modulus, and thermal expansion coefficient, of the monolayers used in this study. Since the density of each monolayer was greater than 3.2 g/cm^3, it was found that each monolayer was fully densified by hot-pressing at 1700°C for 1 h. Furthermore, it appeared that Young's modulus and the thermal expansion coefficient increased with the SiC whisker content. The layered composites had an inner layer of SiC-whisker-reinforced Si_3N_4 composite with a greater coefficient of thermal expansion than the two outer surface Si_3N_4 monolithic layers. Therefore, the outer surface layer was compressed in the direction parallel to the interface after the hot-pressed body was cooled to room temperature.

3.2. Microstructure of layered composite

Figure 1 shows an external view of the layered composite in which the thickness of the surface layers was 200 μm. It was found that the three layers with uniform thickness were stacked after hot-pressing. In this optical micrograph, the Si_3N_4 layer looks white and the layer containing SiC whisker looks gray. When a SiC whisker moves to the surface from an inner layer, the color near the interface

Table 1.
Physical properties of monolayers

	Density (g/cm^3)	Young's modulus (GPa)	Thermal expansion coefficient (10^6)
Si_3N_4	322	303	3.39
Si_3N_4 + 10 wt% SiC whisker	324	320	3.58
Si_3N_4 + 20 wt% S SiC whisker	324	334	3.74

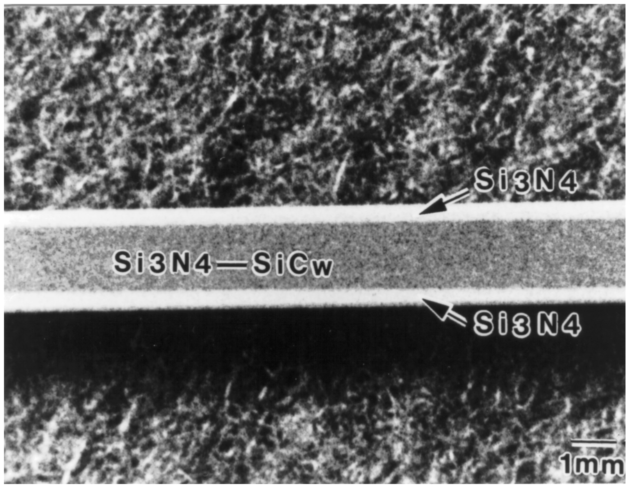

Figure 1. Optical micrograph of a layered composite in which the surface layer thickness is 200 μm.

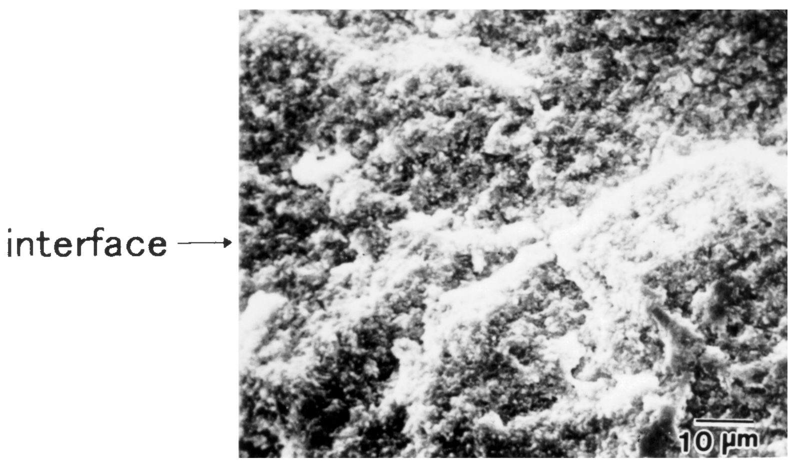

Figure 2. Scanning electron micrograph of the fracture surface around the interface of the layered composite.

changes gradually from white to gray. However, clear interfaces between the surface and inner layers were observed. Therefore, it was thought that there was little movement of SiC whiskers through the interface. Figure 2 shows a scanning electron micrograph of the fracture surface around the interface for the layered composite. It was found that no clear interface was observed, and both the Si_3N_4 monolithic and SiC-whisker-reinforced Si_3N_4 composite layers were tightly joined. This seemed to be because the morphology of Si_3N_4 elongated grain and SiC whisker was nearly the same.

3.3. Surface residual compressive stress

Figure 3 shows the surface residual compressive stress of the layered composite. The closed circles and the open circles indicate the measured values for samples in which the inner layer whisker content is 10 and 20 wt%, respectively. On the other hand, the solid and dashed lines indicate the calculated values for the samples in which the inner layer whisker content is 10 and 20 wt%, respectively. It was found that the measured residual stresses agreed well with the calculated values and decreased with the thickness of the surface layer.

Surface residual compressive stress is influenced by the ratio of surface layer thickness and inner layer thickness. Therefore, if the total thickness is more than 3 mm without changing the surface layer thickness, surface residual compressive stress becomes larger. Furthermore, if the surface layer is smaller than the critical thickness, some cracks are generated at the interface of the layered composite after sintering and surface residual compressive stress is thought to become smaller.

3.4. Mechanical properties of layered composite

In the indentation test, the influence of the inner layer was thought to be very small because the crack length was smaller than the surface thickness. Therefore, the obtained values were regarded as those of the surface Si_3N_4 layers. Figures 4 and 5 show the Vickers hardness and fracture toughness of layered composites as a function of the thickness of the surface layer. It was found that both the Vickers hardness and fracture toughness of the layered composites decreased with the thickness of the surface layer.

In order to discuss the strength of the layered composites, stresses generated in the composite, shown schematically in Fig. 6, were considered in terms of mechanics. The layered composite consists of three layers, with thicknesses h_1, h_2, and h_3 and Young's modulus values E_1, E_2, and E_3, the subscripts 1, 2, and 3 indicating

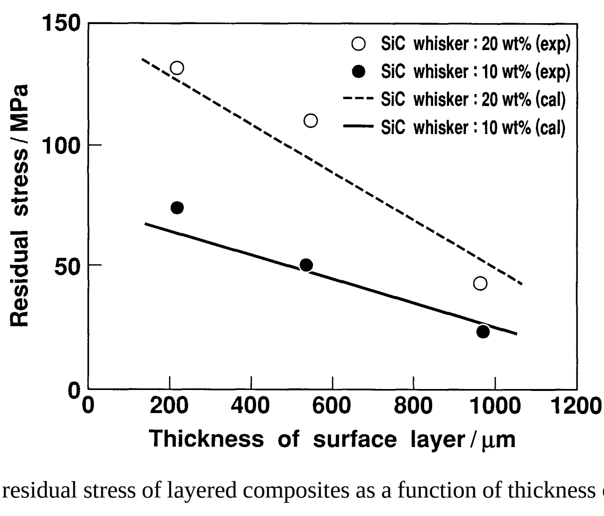

Figure 3. Surface residual stress of layered composites as a function of thickness of the surface layer.

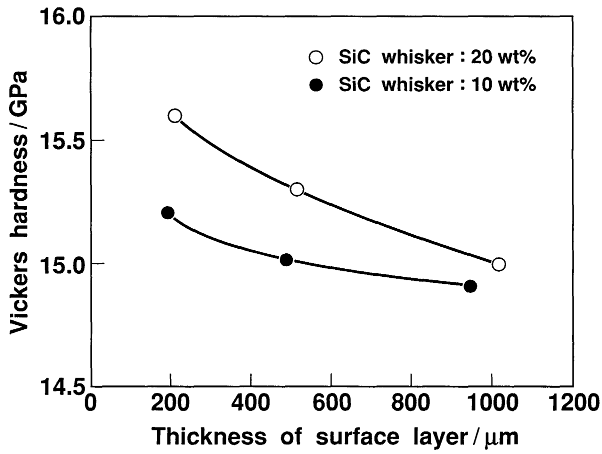

Figure 4. Vickers hardness of layered composites as a function of thickness of the surface layer.

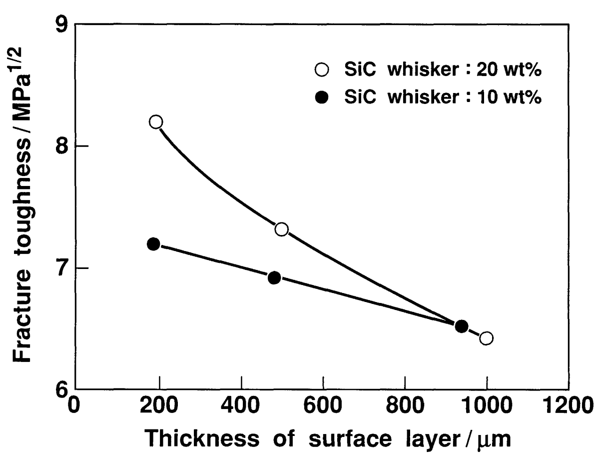

Figure 5. Fracture toughness of layered composites as a function of thickness of the surface layer.

the respective layers. In this flitch beam model, it is assumed that the interface of the layers is tightly bonded and the shear stress is not considered. In this layered composite, surface layers 1 and 3 are Si_3N_4, with the same thickness, and layer 2 is SiC-whisker-reinforced Si_3N_4. When the three-point bending load P is applied to the layered composite with a span of S, because layer 1 is on the tension side (shown in Fig. 6), the stress σ_1 generated at the surface, i.e. the maximum stresses for layer 1, is given by

$$\sigma_1 = \frac{PSE_1\eta}{4(2E_1I_1 + E_2I_2)}, \tag{1}$$

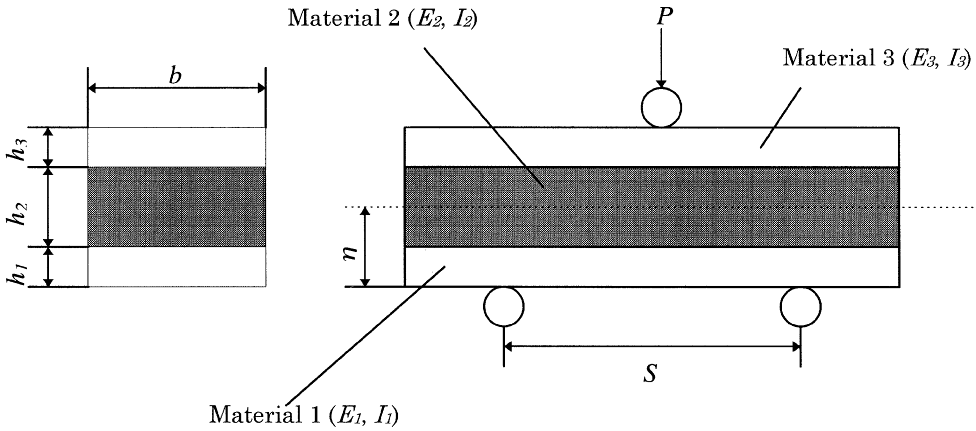

Figure 6. Schematic drawing of a layered composite for strength calculation.

η is the position of the neutral plane on which there is no tensile or compressive stress. It is given by

$$\eta = \frac{2h_1 + h_2}{2}, \tag{2}$$

I_1 and I_2 are moments of inertia of area, which are calculated from

$$I_1 = \frac{bh_1(4h_1^2 + 6h_1h_2 + 3h_2^2)}{12}, \tag{3}$$

$$I_2 = \frac{bh_2^3}{12}, \tag{4}$$

where b is the width of the composite.

The bending strength of the layered composites was calculated from equation (1) assuming that the composites would fracture when σ_1 reached the strength of the monolithic Si_3N_4. The thickness of the composite and the span used in this calculation were the same as those in the experiment (3 and 30 mm, respectively).

Figures 7 and 8 show the bending strength of layered composites as a function of the thickness of the surface layer for samples in which the inner layer whisker content is 10 and 20wt %, respectively. The closed circles indicate the measured values and the solid lines indicate calculated values based on the flitch beam model. It was found that the bending strengths were much higher than the calculated ones and decreased with the surface layer thickness. Moreover, it was found that each mechanical property was affected by the SiC whisker content of the inner layer, that is, the higher the SiC whisker content, the higher the Vickers hardness, fracture toughness, and bending stress. Furthermore, it was found that they showed the same relationship to the thickness of the surface layer as to the surface residual stress.

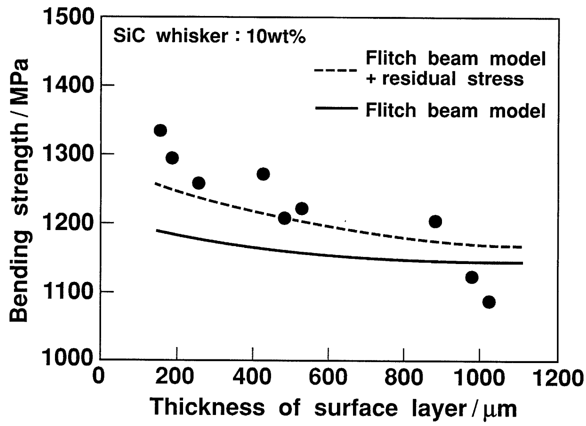

Figure 7. Bending strength of layered composites as a function of thickness of the surface layer (inner layer whisker content is 10wt%).

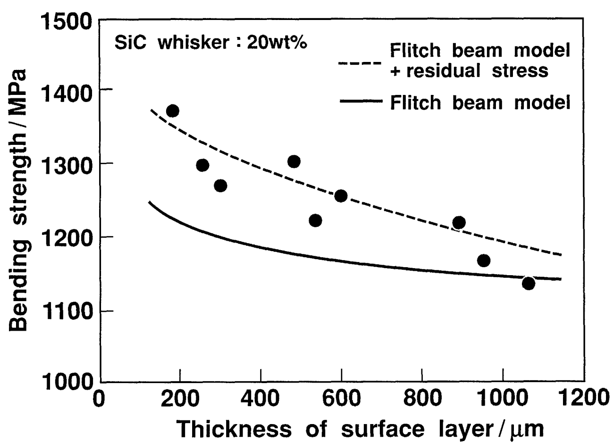

Figure 8. Bending strength of layered composites as a function of thickness of the surface layer (inner layer whisker content is 20wt%).

3.5. Relationship between mechanical properties and compressive stress

The strength of the layered composite was also calculated again in terms of the residual stress, that is, assuming that the composite would fracture when the value of σ_1 plus the residual stress reached the strength of the monolithic Si_3N_4. The other assumptions were the same as for the previous calculation. The results of these calculation are also shown in Figs 7 and 8 as dashed lines. It was found that the values calculated with the residual stress agreed much better with experimental values than the values calculated without the surface residual stress. Therefore, the main cause of the increase in strength is thought to be the compressive residual stress in the surface Si_3N_4 layer.

The surface residual stress also seemed to improve the Vickers hardness and the fracture toughness of the layered composites, because they were calculated from the diagonal length of the indentor trace of and the crack length, which were affected by surface compressive stress.

Therefore, it was thought that the mechanical properties of the layered composites were improved by the surface compressive stress due to the mismatch of thermal expansion between the surface Si_3N_4 layers and the inner SiC-whisker-reinforced Si_3N_4layer.

4. CONCLUSION

The following conclusions were reached based on the results of this investigation.

(1) The Vickers hardness, fracture toughness, and bending strength of Si_3N_4/SiC-whisker-reinforced Si_3N_4 three-layer composites were higher than those of each monolayer.

(2) The surface residual compressive stress decreased with the thickness of the surface layer and also increased with the content of SiC whiskers.

(3) The mechanical properties of the Si_3N_4/SiC-whisker-reinforced Si_3N_4 three-layer composites were improved by the surface compressive stress due to the mismatch of the thermal expansion coefficient between the surface Si_3N_4 layers and the inner SiC-whisker-reinforced Si_3N_4layer.

Acknowledgements

This work was supported by NEDO as a part of the Synergy Ceramics Project under the Industrial Science and Technology Frontier (ISTF) Program promoted by AIST, MITI, Japan. The authors are members of the Joint Research Consortium of Synergy Ceramics.

REFERENCES

1. R. Sathyamoorthy, A. V. Virker and R. A. Cutler, Damage-resistant SiC-AlN layered composites with surface compressive stresses, *J. Amer. Ceram. Soc.* **75**, 1136–1141 (1992).
2. A. V. Virker, J. L. Huang and R. A. Cutler, Strengthening of oxide ceramics by transformation-induced stresses, *J. Amer. Ceram. Soc.* **70**, 164–170 (1987).
3. A. V. Virker, J. F. Jue, J. J. Hansen and R. A. Culeter, Measurement of residual stresses in oxide-ZrO_2 three-layer composites, *J. Amer. Ceram. Soc.* **71**, C148–151 (1988).
4. R. A. Culter, J. D. Bright, A. V. Virker and D. K. Shetty, Strength improvement in transformation-toughened alumina selective phase transformation, *J. Amer. Ceram. Soc.* **70**, 714–718 (1987).
5. H. Wang and X. Hu, Surface properties of ceramic laminates fabricated by die pressing, *J. Amer. Ceram. Soc.* **79**, 443–556 (1996).
6. T. Chartier, D. Merle and J. L. Besson, Laminar ceramic composites, *J. Eur. Ceram. Soc.* **15**, 101–107 (1995).
7. T. Kim, M. F. Amateau and G. L. Messing, Residual stresses in SiC whisker/mullite laminated composites, in: *Advanced Composite Materials*, M. D. Sacks (Ed.), pp. 677–693. ACS, Westerville, Ohio (1996).

8. I. M. Low, R. D. Skala and D. Zhou, Synthesis of functionally gradient aluminium titanate/alumina composites, *J. Mater. Sci. Lett.* **15**, 345–347 (1996).
9. H. Takebe and K. Morinaga, Fabrication and mechanical properties of lamellar Al_2O_3 ceramics, *J. Ceram. Soc. Jpn.* **96**, 1149–1156 (1988).
10. H. Katsuki, H. Ichinose, A. Shiraishi, H. Takagi and Y. Hirata, Preparation and fracture characteristic of laminated alumina/mullite composites, *J. Ceram. Soc. Jpn.* **101**, 1068–1070 (1993).
11. M. J. Melendo, C. Cluss and A. D. Rodriguez, Microstructure and high-temperature mechanical behavior of alumina/alumina-yttria-stabilized Tetragonal zirconia multilayer composites, *J. Amer. Ceram. Soc.* **80**, 2126–2130 (1997).
12. H. Liu, B. R. Lawn and S. M. Hsu, Contact response of tailored silicon nitride multilayers, *J. Amer. Ceram. Soc.* **79**, 1009–1014 (1996).
13. P. Z. Sajgalik, Lences and J. Dusza, Layered Si_3N_4 composites with enhanced room temperature properties, *J. Mater. Sci.* **31**, 4837–4842 (1996).
14. H. Liu and S. M. Hsu, Fracture behavior of multilayer silicon nitride/boron nitride ceramics, *J. Amer. Ceram. Soc.* **79**, 2452–2457 (1996).
15. Y. Shigegaki, M. E. Brito, K. Hirao, M. Toriyama and S. Kanzaki, Processing of a novel multilayered silicon nitride, *J. Amer. Ceram. Soc.* **79**, 2197–2200 (1996).
16. T. Fukasawa and Y. Goto, Fracture behavior of SiC whisker/Si3N4 multi-layered composites, *J. Mater. Sci. Lett.* **16**, 1423–1425 (1997).
17. Y. Goto, T. Fukasawa and M. Kato, Strength of β-sialon/Si_3N_4 layered composites, *J. Mater. Sci.* **33**, 423–427 (1998).
18. Y. Goto, T. Fukasawa, M. Kato, S. Suyama and T. Kameda, Fabrication and mechanical properties of layered composites, in: *Extended Abstracts of 1st International Workshop on Synergy Ceramics*, pp. 40–41 (1996).
19. T. Fukasawa, Y. Goto, M. Kato, S. Suyama and T. Kameda, Fabrication and mechanical properties of silicon-carbide-based layered composites, in: *Proc. 6th Intern. Symp. on Ceramic Materials and Components for Engines*, pp. 289–293 (1997).
20. S. A. Bradley, K. R. Karasek, M. R. Martin and H. C. Yeh, Silicon carbide whisker stability during processing of silicon nitride matrix composites, *J. Amer. Ceram. Soc.* **73**, 628–636 (1989).
21. Y. Goto and A. Tsuge, Mechanical properties of Si_3N_4-SiC whisker composites, in: *Proc. 9th Symp. on Basic Technology for Future Industries, Fine Ceramics Research Association*, pp. 147–154 (1991).